A coupled hydromechanical fault model for the study of the integrity and safety of geological storage of CO2

Ariane Ducellier, Darius Seyedi, Evelyne Foerster

HAL Id: hal-00560485

https://brgm.hal.science/hal-00560485

Submitted on 28 Jan 2011

A coupled hydromechanical fault model for the study of the integrity and safety of geological storage of CO_2

Ariane Ducellier[1], Darius Seyedi[1], Evelyne Foerster[1]

[1] BRGM, Natural Risks & CO_2 Storage Security Division, 3 av. C. Guillemin, BP 36009, 45060 Orléans Cedex 2, France

Abstract

The safety study of a CO_2 storage site requires the evaluation of the sustainable injection pressure. The faults are generally considered as one of the potential leakage paths as a fault zone could be more permeable than the neighbouring rock matrix. The pressure build up in the reservoir due to the injection procedure changes the stress field within the reservoir and its surrounding rocks. The decrease of effective stress in the vicinity of a fault, due to this pore pressure increase, may lead to fault failure, increasing its permeability or even creating induced seismicity. The aim of this study is to carry out large-scale 2D coupled hydromechanical simulations of the fault behaviour during and after the injection and to study the sensibility of the fault response regarding to some parameters.

1. Introduction

From a practical point of view, the safety study of a CO_2 storage site consists, among others, in the evaluation of the sustainable injection pressure. Gas injection modifies the reservoir pressure and decreases the effective stress field (soil mechanics convention) in the reservoir and the cap rock formations, which may lead toward the failure of faults embedded in the reservoir, increasing permeability of the fault zone or even creating induced seismicity. One simple way of evaluating the risk of fault reactivation is to model the effective stress field in the reservoir, to compute shear and normal stresses of a cohesionless fault in function of the fault dip and to compare them to a fault reactivation criterion (e.g. [1; 2; 3]). However, this approach does not allow taking into account the effects of the presence of the fault on the stress field in the surrounding rock matrix. Moreover, the permeability contrast between a faulted zone and the neighbouring rock matrix is generally high. If the faulted zone runs across the reservoir and the cap rock, it may create a preference leakage path leading to the contamination by the CO_2 of the aquifers located above the cap rock. A more accurate fault modelling is then required. An approach using continuum stress-strain analysis or discrete fault analysis has been developed for instance by [4].

The objective of the present work is to describe more accurately a single fault running across the reservoir and to model its hydromechanical behaviour by a specific model implemented within the finite elements code Gefdyn [5; 6]. As a first order approximation, a fault is modelled as a thin layer of filling material different from the neighbouring rock matrix, surrounded on both sides by a series of hydromechanical joint elements. The hydromechanical response of the fault depends on the permeability of the filling material: with a low permeability (e.g. as low as that of the cap rock), the fault behaves as a hydraulic seal; with a high permeability (e.g. as high as that of the reservoir), the fault behaves as a hydraulic conduct. Furthermore, the joint elements allow modelling the slip or the opening of the fault due to effective stress change during gas injection operation and storage period. The joint elements approach consists in using a consistent formulation of flow in deformable rock

masses through a variational formulation, as the rock deformations and the fluid are fully coupled.

Two effects of CO_2 injection on the hydromechanical behaviour of the fault are then observed. First, the fluid flow at the boundary between the cap rock and an upper aquifer is observed at the level of the fault. Second, the Mohr-Coulomb failure criterion is considered to characterize fault failure possibility. A quick sensibility analysis is then carried out to determine which parameters have the most influence on the fault response. Finally, the evolution of the fluid flow when the injection pressure and the permeability of the filling material vary and the occurrence of fault failure when the injection pressure and the fault friction angle or the initial stress state vary, are studied.

2. Reference scenario

A set of large-scale two-dimensional coupled hydromechanical calculations is performed to demonstrate the developed model capacities. Considering that the affected fault is located at a reasonable distance from the injection well, the CO_2 injection is modelled as a pore pressure increase within the reservoir. The stocking process is simulated in two steps. First, an increasing pore pressure is imposed along a vertical line running across the reservoir, simulating the injection well during the injection period. The fluid pressure imposed at the injection well level is equal to the hydrostatic pressure at the beginning of the simulation and then varies linearly to a maximum value. Second, the system is set free and the fluid flow along the reservoir and across the fault is observed. This corresponds to the storage period.

To illustrate this simulation procedure, we have applied it to a representative potential site based on the Dogger aquifer of the Paris basin [7; 8]. The Paris basin is a multilayered system, which consists of several layers of permeable brine-water formations (denoted "aquifers") separated by less permeable formations. In order to simplify the geological model [3], all layers are assumed horizontal. A total number of five aquifer layers have been taken into account, namely (from the soil surface): the chalk aquifer of the Upper Cretaceous geological unit, the sandstone aquifer of the Albian geological unit, the carbonate aquifer of the Lower Cretaceous geological unit, the carbonate aquifer of the Oxfordian and Kimmeridgian geological units and the target carbonate aquifer of the Dogger geological unit. The tertiary formations have not been taken into account. Clay and shale layers of low permeability interlace these formations (denoted "aquitard"). The depth and thickness of each layer are based on the mean values, which can be found in the Paris basin [8]. A schematic view of the model is given in Figure 1 and the soil layers are described in Table 1.
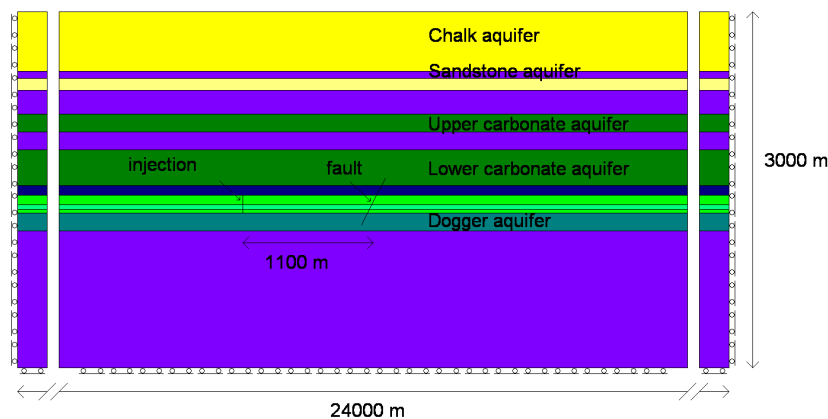
Figure 1: Schematic view of the Paris basin model

The hydraulic and mechanical properties of the various materials are described in Table 1. Hydraulic properties are determined based on previous works [7 - 16]. Rock bulk density is set to 2500 kg.m^{-3} for all the soil layers and an at-rest lateral earth pressure of 0.75 is chosen [17].

The geological model used is represented as a rectangle of 3000 m depth and 24000 m width. It is crossed in its middle by a fault of ~63° dip. The fault runs across the Dogger reservoir, the cap rock and the lower carbonate aquifer and its extremities are located at 1400 and 1800 m depth respectively (Figure 1). The injection well is located in the Dogger reservoir (between 1550 and 1700 m depth). 1100 meters separate the fault from the injection point. On the left, right and lower boundaries, a null normal displacement is imposed. On the left and right boundaries, we impose a hydrostatic pressure.

Table 1: Thicknesses and hydromechanical properties of the Paris basin soil layers.

Layer name	Thickness (m)	Depth (m)	Young modulus (GPa)	Poisson ratio	Porosity (%)	Permeability (m.s^{-1})
Chalk aquifer	500	500	5	0.3	30	9.81 10^{-9}
Clay formation	60	560	6.65	0.285	5	9.81 10^{-12}
Sandstone aquifer	100	660	10	0.3	25	4.905 10^{-4}
Clay formation	200	860	6.65	0.285	5	9.81 10^{-12}
Upper carbonate aquifer	150	1010	15	0.3	15	9.81 10^{-7}
Clay formation	150	1160	6.65	0.285	5	9.81 10^{-12}
Lower carbonate aquifer	300	1460	20	0.3	15	9.81 10^{-7}
Cap rock	90	1550	6.65	0.285	5	4.905 10^{-13}
Dogger aquifer (low permeability)	80	1630	24	0.29	15	8.829 10^{-7}
Dogger aquifer (high permeability)	40	1670	24	0.29	15	6.916 10^{-6}
Dogger aquifer (low permeability)	30	1700	24	0.29	15	8.829 10^{-7}
Lower Dogger	150	1850	42	0.29	10	9.81 10^{-9}
Clay formation	1150	3000	6.65	0.285	5	9.81 10^{-12}

A specific fault model is considered. It consists of a double set of joint elements filled by a porous material. The filling material will allow the fault to behave as a hydraulic conduct or seal, depending of the lower or higher material permeability. This material layer is surrounded on each side by two series of joint elements [18], which will allow simulating a slip or an

opening of the fault (Figure 2). The hydraulic and mechanical parameters of the joint elements are described in Table 2.
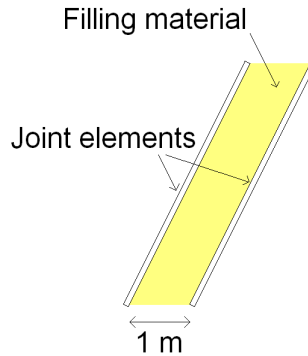

Figure 2: Schematic view of the fault model

Table 2: Joint elements parameters

Parameter	Value
Normal stiffness	100 GPa/m
Tangential stiffness	10 GPa/m
Initial opening	10^{-3} m
Minimal opening	10^{-4} m
« Permeability (k_f) »	6.916 $m^{-1}.s^{-1}$
Cohesion	0 Pa
Friction angle	30°

The fluid flow in the fracture follows a square law that can be defined by:

$$\partial_t \overrightarrow{u_{rw}} = -K_f \overrightarrow{grad(p)} \quad \text{where} \quad K_f = k_f e^2 / 12\rho g \tag{1}$$

where $\partial_t u_{rw}$ is the velocity of the fluid relative to the solid, p, the fluid pressure, k_f the fault permeability, e the opening of the fracture, ρ, the bulk fluid density and g, the gravity.

Four scenarios are studied: (1) the filling material permeability is equal to the cap rock permeability; (2) the filling material permeability is ten times lower than the cap rock permeability; (3) the filling material permeability is equal to the reservoir permeability and (4) the filling material permeability is ten times higher than the reservoir permeability. In the first two cases, the fault behaves like a hydraulic seal. In the two last ones, the fault behaves as a hydraulic conduct. The Young modulus of the filling material is equal to 6.65 GPa; its Poisson ratio is equal to 0.285 and its porosity is equal to 5 %. The considered time step is 5 10^5 seconds (around 5.79 days). The injection duration is 500 time steps (around 7.93 years). At the end of the injection, the imposed fluid pressure at the well level is equal to 1.5 times the initial pressure. The fault behaviour evolution after the end of the injection during 500 time steps is also observed.

We observe the evolution of the fluid flow in the fracture at the interface between the cap rock and the lower carbonate aquifer in function of the time (Figure 3). The pressure increase at the well level increases the pressure gradient and consequently the flow along the fault, leading to

a fluid rising from the reservoir to the aquifer above the cap rock. A connection thus can be made between the target reservoir and an upper aquifer, inducing its contamination. We note that, when the filling material permeability is close to the reservoir permeability, the flow at the interface between the cap rock and the lower carbonate aquifer is very important. The fault behaves actually as a conduct. When the filling material permeability is close to the cap rock permeability, the flow is much lower. The fault behaves as a hydraulic seal.
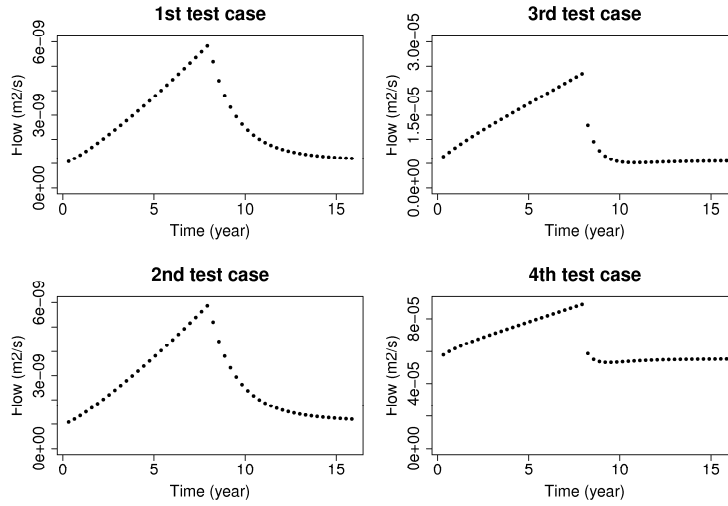

Figure 3: Evolution of fault fluid flow for four different filling material permeability values

The increase of effective stress due to the increase of fluid pressure can lead to a slip rupture. The risk of fault reactivation is evaluated with the Mohr-Coulomb failure criterion [19]:

$$\left| \sigma_T' \right| + \sigma_N' \tan \varphi - c > 0 \tag{2}$$

where σ'_T and σ'_N are shear and normal stresses, φ, the friction angle and c, the cohesion of the joint element. As we are studying the fault reactivation risk, we suppose the cohesion is null. A friction angle equal to 30° is considered. It can be noticed that the Mohr-Coulomb failure criterion is not reached for any of the four scenarios. There is no fault reactivation due to the CO_2 injection for the set of parameters taken in the reference scenario.

3. Sensibility analysis

To study the sensibility of the fault response regarding to the different hydromechanical parameters of the model, a reference test case is defined, and then each parameter is tested individually. A range of variation for each parameter is considered and two computations are then carried out: a first one with the minimum value this parameter can take and a second one with the maximum value.

The parameters chosen for the sensibility analysis are the hydromechanical parameters (Young modulus, Poisson ratio, porosity and permeability) of the layers surrounding the fault (lower carbonate aquifer, cap rock, low permeable Dogger, high permeable Dogger, lower Dogger and fault filling material), the initial stress state (at-rest lateral earth pressure), rock density, and the hydromechanical parameters of the joint elements (normal and tangential stiffness, cohesion, friction angle, permeability, initial opening, minimal opening). For the Young modulus, Poisson ratio and porosity of the material layers, the maximum and

minimum values are respectively 1.5 and 0.5 times the reference value given in Table 1. As the permeability values are less accurately known, we assume a maximum value of 10 times the reference value and a minimum one of 0.1 times the reference value for this parameter. The uncertainty regarding the other model parameters is more important, thus a wider range of value is tested. The maximum, minimum and reference values of these parameters are given in Table 3.

Table 3: Maximum and minimum values of model parameters used in the sensibility analysis

Parameters		Reference value	Minimum value	Maximum value
Filling material	Young modulus (GPa)	20	5	35
	Poisson ratio	0.3	0.15	0.45
	Porosity (%)	10	2.5	17.5
	Permeability (m.s^{-1})	$9.81\ 10^{-9}$	$4.905\ 10^{-14}$	$6.916\ 10^{-5}$
Stress state	At-rest lateral earth pressure	0.75	0.6	1.2
	Bulk density (kg.m^{-3})	2500	2200	2800
Joint elements parameters	Normal stiffness (GPa/m)	100	10	1000
	Tangential stiffness (GPa/m)	10	1	100
	Cohesion (Pa)	0	0	10^{6}
	Friction angle (°)	30	10	60
	Permeability (m^{-1}.s^{-1})	$9.81\ 10^{-3}$	$4.905\ 10^{-8}$	69.16
	Initial opening (m)	10^{-3}	10^{-4}	10^{-2}
	Minimal opening (m)	10^{-4}	10^{-4}	10^{-2}

The flow and the Mohr-Coulomb failure criterion (cf. Eq. 2) at the level of the interface between the reservoir and the cap rock on the fault side nearest from the injection well are investigated. Figure 4 presents the flow variation along the fault at the end of the injection (left) and 500 time steps after the end of the injection (right) for the following parameters: filling material permeability (K_m), high permeable Dogger permeability (K_d), fault permeability (K_f), joint elements initial opening (e). The triangles correspond to the minimum tested value, the squares to the maximum value and the circles to the reference value. We observe that the main influence on the flow comes from the filling material permeability. However, the reservoir permeability (high permeable Dogger) and the permeability and initial opening of joint elements have also a non neglectable effect, while the remaining parameters have little effect.
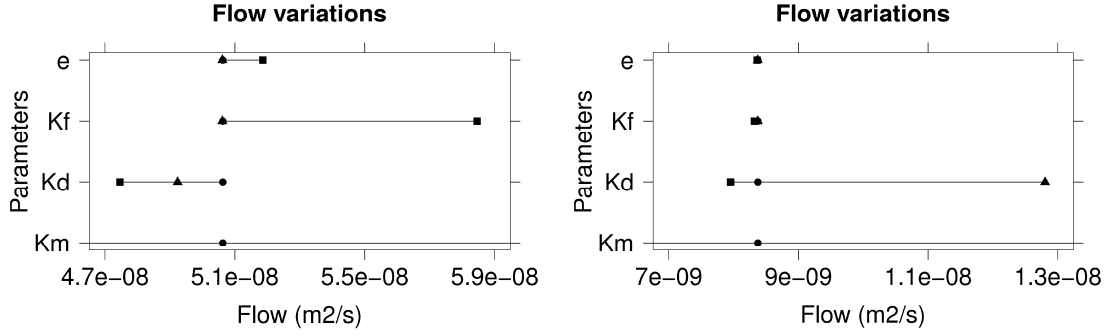
Figure 4: Comparison of parameters effect on the flow

Figure 5 presents the Mohr-Coulomb criterion variation at the end of injection (left) and 500 time steps after the end of injection (right) for the following parameters: rock density (rho), at-rest lateral earth pressure (K0), friction angle (phi), normal stiffness (K). On this figure, we see that the friction angle and the lateral stress ratio have a preponderant influence on the failure criterion. The rock density and the normal stiffness have also an important effect, while the other parameters seem to be of less influence.
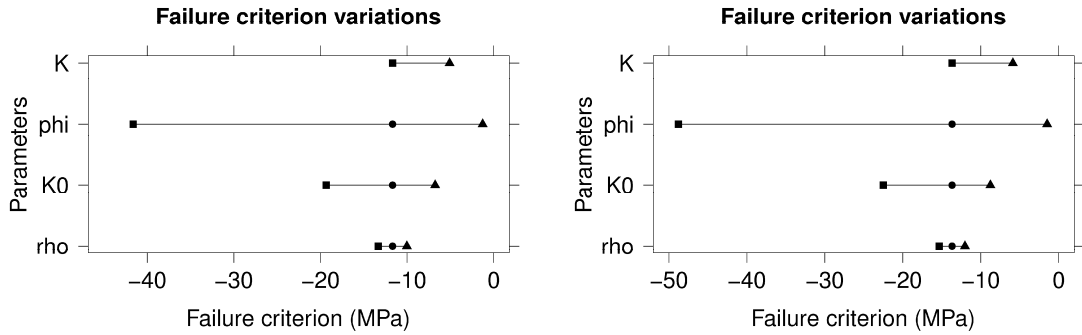

Figure 5: Comparison of parameters effect on the Mohr-Coulomb failure criterion

4. Further sensibility analysis

The evolution of the flow along the fault at the interface between the cap rock and the lower carbonate aquifer is studied while the maximum injection pressure and the parameter having the main influence on the flow (i.e. the filling material permeability) vary. The maximum injection pressure varies between 1 and 2 times the initial pressure. The filling material permeability varies between $4.905 \ 10^{-14}$ m/s (10 times less than the cap rock permeability) and $6.916 \ 10^{-5}$ m/s (10 times more than the reservoir permeability).

In the following section, we investigate the flow value (q) along the fault at the interface between the cap rock and the lower carbonate aquifer against the maximum vs. initial pressure ratio (R_p) and the filling material permeability (k) at the end of the injection period, as well as 500 time steps after the end of the injection. A least-squares linear regression allows us to verify that the logarithm of the flow varies linearly against R_p and the logarithm of k:

$$\log(q) = \beta_0 + \beta_1 R_P + \beta_2 \log(k) \qquad (3)$$

The values of the regression coefficients β_i (i = 0, 1, 2) are given in Table 4. The quality of the linear regression is evaluated by cross validation [20]. This method consists in removing a couple of data from the initial data set, doing again the regression with the new data set and estimating the value of the removed couple of data with the regression formula then obtained. This operation is done with all couples of data of the initial data set. The quality of the regression is then evaluated with the determination coefficient R^2. Regression coefficient R² is close to one for both cases. The linear regression models thus correctly the flow along the fault.

Table 4: Linear regression coefficients

Model variable	β_0	β_1	β_2	R^2
Flow at the end of the injection	-0.815	0.836	0.993	0.995
Flow 500 time steps after the end of the injection	-0.222	0.065	0.993	1.000

The evolution of the Mohr-Coulomb failure criterion is then studied while the maximum injection pressure and the parameter which has the more influence on the failure criterion (i.e. the joint elements friction angle) vary. The maximum injection pressure varies between 1 and 2 times the initial pressure. The friction angle varies between 10° and 40°. The permeability of fault filling material is supposed to be equal to the reservoir permeability. We check then if the Mohr-Coulomb failure criterion is reached or not during the injection or after the injection.

A failure is observed only for a friction angle of 10° and a maximum injection pressure higher than 1.5 times the initial pressure. We note that when the joint elements friction angle becomes low and the ratio between maximum and initial injection pressure increases, the risk of a failure increases following the Mohr-Coulomb criterion.

Finally, the failure possibility is studied while the maximum injection pressure and another influential parameter, e.g. the at-rest lateral earth pressure coefficient, vary. The maximum injection pressure varies between 1 and 2 times the initial pressure. The ratio between horizontal and vertical stresses varies between 0.6 and 1.2. We assume the filling material permeability to be equal to the reservoir permeability. The friction angle of the joint elements is equal to 30°. In the range of values chosen to carry out the series of simulations, the Mohr-Coulomb failure criterion is never reached, neither during the injection nor after the injection.

5. Conclusion

The hydromechanical behaviour of a fault running across a reservoir during a CO_2 injection scenario has been modelled and the influence of some of the model parameters on the fracture response has been studied. A fast sensibility study allows to show that the parameters which have the most influence on the flow along the fault are the filling material permeability as well as, in a lower extent, the reservoir permeability, the joint elements permeability and the initial opening of the joint elements. The parameters which have the greatest influence on the Mohr-Coulomb failure criterion and hence, possible fault reactivation, are the at-rest lateral earth pressure coefficient, the friction angle of the joint elements, as well as, in a lower extent, the rock density and the normal stiffness of the joint elements. When the friction angle is low or when the injection pressure increases, we notice that a fault reactivation becomes possible. No fault reactivation is observed by making the at-rest lateral earth pressure coefficient vary, for the set of considered parameters.

References

[1] Rutqvist J, Birkholzer JT, Tsang CF. Coupled reservoir-geomechanical analysis of the potential for tensile and shear failure associated with CO_2 injection in multilayered reservoir-caprock systems. Int. J. Rock Mechanics & Mining Sciences 2008;45:132-43.

[2] Soltanzadeh H, Hawkes CD. Semi-analytical models for stress change and fault reactivation induced by reservoir production and injection. J. Petroleum Science & Engineering 2008;60:71-85.

[3] Rohmer J, Seyedi DM. Coupled large scale hydromechanical modelling for caprock failure risk assessment of CO_2 storage in deep saline aquifers. Oil & Gas Science and Technology – Rev. IFP 2010;65:503-517.

[4] Rutqvist J, Birkholzer J, Cappa F, Tsang CF. Estimating maximum sustainable injection pressure during geological sequestration of CO_2 using coupled fluid flow and geomechanical fault-slip analysis. Energy Conversion and Management 2007;48:1798-807.

[5] Aubry D, Chouvet D, Modaressi A, Modaressi H. GEFDYN : Logiciel d'analyse de comportement mécanique des sols par éléments finis avec prise en compte du couplage sol-eau-air. Manuel scientifique. Paris: Ecole Centrale Paris LMSS-Mat; 1986.

[6] Aubry D, Modaressi A. GEFDYN. Manuel scientifique. Paris: Ecole Centrale Paris LMSS-Mat; 1996.

[7] Brosse E, Hasanov V, Bonijoly D, Garcia D, Rigollet C, Munier G et al. The PICOREF Project: Selection of geological sites for pilot CO_2 injection and storage in the Paris basin. In: Proceedings of the 1st French German Symposium on Geological Storage of CO_2, 21-22 June 2007, Potsdam, Germany.

[8] Grataloup S, Bonijoly D, Brosse E, Garcia D, Hasanov V, Lescanne M et al. PICOREF: A site selection methodology for saline aquifer in Paris basin. In: Proceedings of the 9th International Conference on Greenhouse Gas Technologies, 16-20 November 2008, Washington, USA.

[9] Rojas J, Giot D, Le Nindre YM, Criaud A, Fouillac C, Brach M. Caractérisation et modélisation du réservoir géothermique du Dogger, bassin parisien, France. Technical report CCE, EN 3G-0046-F(CD), BRGM R 30 IRG SGN 89, 1989.

[10] ANDRA. Dossier 2005 Argile - Synthèse : Evaluation de la faisabilité du stockage géologique en formation argileuse. Rapport ANDRA – Reference 266, 2005.

[11] Fleury M. The GeoCarbone - Integrity program: Evaluating sealing efficiency of caprocks for CO_2 storage. In: Proceedings of the 1st French German Symposium on Geological Storage of CO_2, 21-22 June 2007, Potsdam, Germany.

[12] Freissmuth H. The influence of water on the mechanical behaviour of argillaceous rocks. PhD thesis. Paris: Ecole Nationale Supérieure des Mines de Paris; 2002.

[13] Bounenni A. Etude expérimentale de l'effet d'endommagement sur la perméabilité des roches. PhD thesis. Paris: Ecole Nationale des Ponts et Chaussées; 2002.

[14] Vidal-Gilbert S, Huguet F, Assouline L, Longuemare P. Hydromechanical modelling of reservoir behaviour during underground gas storage exploitation. In: Proceedings of the 67th EAGE Conference & Exhibition, 13-16 June 2005, Madrid, Spain.

[15] Vidal-Gilbert S. Bemer E, Barroux C, Brosse E. Hydromechanical behaviour during CO_2 injection. In: Proceedings of the ISRM Regional Symposium Eurock 2006, 9-12 May 2006, Liège, Belgium.

[16] Bemer E, Lombard JM. Caractérisation expérimentale de l'évolution des propriétés géomécaniques de roches carbonatées sous l'effet d'une altération géochimique homogène. In: Captage et Stockage du CO_2, Colloque ANR 2007, 12-13 December 2007, Pau, France.

[17] Cornet FH, Burlet D. Stress field determinations in France by hydraulic test in borehole. J. Geophys. Res. 1992;97:11829-49.

[18] Modaressi H, Aubry D. Numerical modelling for the flow of compressible fluids in systems of deformable fractured rocks. In: Numerical Models in Geomechanics - Numog III. Elsevier Applied Science; 1989, p. 391-398.

[19] Morris A, Ferril DA, Henderson DB. Slip tendency analysis and fault reactivation. Geology 1996;24:275-8.

[20] Hjorth JSU. Computer intensive statistical methods: Validation model selection and bootstrap. London: Chapman and Hall; 1994.